Measuring the spatiotemporal electric field of tightly focused ultrashort pulses with sub-micron spatial resolution.

Pamela Bowlan,[1] Ulrike Fuchs,[2] Rick Trebino[1] and Uwe D. Zeitner[2]

[1]Georgia Institute of Technology, School of Physics,
837 State St NW, Atlanta, GA 30332, USA
[2]Fraunhofer-Institut für Angewandte Optik und Feinmechanik,
Albert-Einstein-Str. 7, 07745 Jena, Germany
PamBowlan@gatech.edu

Abstract: We demonstrate a powerful and practical spectral interferometer with near-field scanning microscopy (NSOM) probes for measuring the spatiotemporal electric field of tightly focused ultrashort pulses with high spatial and spectral resolution. Our measurements involved numerical apertures as high as 0.44 and yielded the spatiotemporal field at and around the foci produced by two microscope objectives and several different lenses. For the first time, we measure the spatiotemporal field of the Bessel-like X-shaped pulse caused by spherical aberrations and a "fore-runner pulse" due to chromatic aberrations. We observed spatial features smaller than 1μm and verified these results with non-paraxial simulations.

References and links

1. Zs. Bor, "Distortion of femtosecond laser pulses in lenses and lens systems," J. Mod. Opt. **35**, 1907-1918 (1988).
2. Z. Bor, "Distortion of femtosecond laser pulses in lenses," Opt. Lett. **14**, 119-121 (1989).
3. Zs. Bor and Z. L. Horvath, "Distortion of femtosecond pulses in lenses. Wave optical description," Opt. Commun. **94**, 249-258 (1992).
4. M. Kempe, U. Stamm, B. Wilhelmi, and W. Rudolph, "Spatial and temporal transformation of femtosecond laser pulses by lenses and lens systems," J. Opt. Soc. Am. B **9**, 1158-1165 (1992).
5. M. Kempe and W. Rudolph, "Femtosecond pulses in the focal region of lenses," Phys. Rev. A **48**, 4721-4729 (1993).
6. Simin Feng and Herbert G. Winful, "Spatiotemporal structure of isodiffracting ultrashort electromagnetic pulses," Phys. Rev. E **61**, 862-873 (2000).
7. P. Saari, "Evolution of subcycle pulses in nonparaxial Gaussian beams," Opt. Express **8**, 590-598 (2001).
8. U. Fuchs, U. D. Zeitner, and A. Tuennermann, "Ultra-short pulse propagation in complex optical systems," Opt. Express **13**, 3852-3861 (2005).
9. Z. L. Horvath and Zs. Bor, "Diffraction of short pulses with boundary diffraction wave theory," Phys. Rev. E **63**, 1-11 (2001).
10. P. Saari, K. Reivelt, and H. Valta, "Ultralocalized Superluminal Light Pulses," Laser Phys. **17**, 297-301 (2007).
11. R. Trebino, *Frequency-Resolved Optical Gating: The Measurement of Ultrashort Laser Pulses* (Kluwer Academic Publishers, Boston, 2002).
12. R. Chadwick, E. Spahr, J. A. Squier, and C. G. Durfee, "Fringe-free, background-free, collinear third-harmonic generation frequency-resolved optical gating measurements for multiphoton microscopy," Opt. Lett. **31**, 3366-3368 (2006).
13. J. Jasapara and W. Rudolph, "Characterization of sub-10-fs pulse focusing with high-numerical-aperture microscope objectives," Opt. Lett. **24**, 777-779 (1999).
14. W. Amir, T. A. Planchon, C. G. Durfee, J. A. Squier, P. Gabolde, R. Trebino, and M. Mueller, "Simultaneous visualizations of spatial and chromatic abberations by two-dimensional Fourier transform spectral interferometry," Opt. Lett. **31**, 2927-2929 (2006).
15. P. Gabolde and R. Trebino, "Single-shot measurement of the full spatio-temporal field of ultrashort pulses with multi-spectral digital holography," Opt. Express **14**, 11460-11467 (2006).

16. M .L. M. Balistreri, H. Gersen, J. P. Korterik, L. Kuipers, and N. F. van Hulst, "Tracking Femtosecond Laser Pulses in Space and Time," Science **294**, (2001).
17. M. L. M Balistreri, J. P. Korterik, L. Kuipers, and N. F. van Hulst, "Phase Mapping of Optical Fields in Integrated Optical Waveguide Structures," J. Lightwave Technol. **19**, 1169 (2001).
18. H. Gersen, E. M. H. P. van Dijk, J. P. Korterik, N. F. van Hulst, and L. Kuipers, "Phase mapping of ultrashort pulses in bimodal photonic structures: A window on local group velocity dispersion," Phys. Rev. E **70**, 066609 (2004).
19. H. Gersen, J. P. Korterik, N. F. van Hulst, and L. Kuipers, "Tracking ultrashort pulses through dispersive media: Experiement and theory," Phys. Rev. E **68**, 026604 (2003).
20. P. Bowlan, P. Gabolde, M. A. Coughlan, R. Trebino, and R. J. Levis, "Measuring the spatiotemporal electric field of ultrashort pulses with high spatial and spectral resolution," J. Opt. Soc. Am. B **25**, A81-A92 (2008).
21. P. Bowlan, P. Gabolde, and R. Trebino, "Directly measuring the spatio-temporal electric field of focusing ultrashort pulses," Opt. Express **15**, 10219-10230 (2007).
22. P. Bowlan, P. Gabolde, A. Schreenath, K. McGresham, and R. Trebino, "Crossed-beam spectral interferometry: a simple, high-spectral-resolution method for completely characterizing complex ultrashort pulses in real time," Opt. Express **14**, 11892-11900 (2006).
23. Cl. Froehly, A. Lacourt, and J. Ch. Vienot, "Time Impulse Responce and time Frequency Responce of Optical Pupils," Nouvelle Revue D'Optique **4**, 183-196 (1973).
24. A. C. Kovaecs, K. Osvay, Bor, Zs, "Group-delay measurement on laser mirrors by spectrally resolved white-light interferometry," Opt. Lett. **20**, 788-791 (1995).
25. K. Misawa and T. Kobayashi, "Femtosecond Sangac interferometer for phase spectroscopy," Opt. Lett. **20**, 1550-1552 (1995).
26. D. Meshulach, D. Yelin, and Y. Silberberg, "Real-Time Spatial-Spectral Interference Measurements of Ultrashort Optical Pulses," J. Opt. Soc. Am. B **14**, 2095-2098 (1997).
27. J. P. Geindre, P. Audebert, S. Rebibo, and J. C. Gauthier, "Single-shot spectral interferometry with chirped pulses," Opt. Lett. **26**, 1612-1614 (2001).
28. E. Betzig, M. Isaacson, and A. Lewis, "Collection mode near-field scanning optical microscopy," Appl. Phys. Lett. **51**, 2088-2090 (1987).
29. E. Betzig, J. K. Trautman, T. D. Harris, J. S. Weiner, and R. L. Kostelak, "Breaking the Diffraction Barrier: Optical Microscopy of a Nanometer Scale," Science **251**, 1468-1470 (1991).
30. Y. H. Fu, F. H. Ho, W. C. Lin, W. C. Liu, and D. P. Tsau, "Study of the focused laser spots generated by various polarized laser beam conditions," J. Microsc. **201**, 225-228 (2002).
31. I. P. Radko, S. I. Bozhevolnyi, and N. Gregersen, "Transfer funcion and near-field detection of evanescent waves," Appl. Opt. **45**, 4054-4061 (2006).
32. B. A. Nechay, U. Siegner, M. Achermann, H. Bielefeld, and U. Keller, "Femtosecond pump-probe near-field optical microscopy," Rev. Sci. Instrum. **70**, 2758-2764 (1999).
33. A. Lewis, U. Ben-Ami, N. Kuck, G. Fish, D. Diamant, L. Lubovsky, K. Lieberman, S. Katz, A. Saar, and M. Roth, "NSOM the Fourth Dimension: Integrating Nanometric Spatial and Femtosecond Time Resolution," Scanning **17**, 3-10 (1995).
34. P. Gabolde, D. Lee, S. Akturk, and R. Trebino, "Describing first-order spatio-temporal distortions in ultrashort pulses using normalized parameters," Opt. Express **15**, 242-251 (2007).
35. "OSLO Optical Design Program," (Lambda Research Corporation, 2004).

1. Introduction

Theoretical studies have shown that very complicated distortions can occur when ultrashort pulses are focused due to commonly occurring, and difficult-to-avoid lens aberrations[1-8]. For example, the presence of an additional pulse well ahead of the main pulse—the so called "fore-runner pulse" or "boundary-wave pulse"—has been predicted to occur at the focus when chromatic aberrations are present and the lens is overfilled[3, 9]. Calculations have also shown that severe spherical aberrations result in Bessel-like pulses (meaning that they have similar properties to "x pulses" such as those described in [10]), which have spatiotemporal intensities shaped like an "X"[5, 8]. Other effects such as radially varying group-delay dispersion, or a pulse that is more chirped at its center than on its sides, are expected to occur at the foci of some lenses. Because focused-pulse distortions are usually spatiotemporal and so require a spatiotemporal measurement technique simultaneously having submicron spatial resolution, femtosecond temporal resolution, and high spectral resolution, many of these distortions have never been directly observed.

Indeed, the focus is a very important place to measure a pulse because this is where most experiments take place so the quality of experiments often greatly depends on the pulse's properties there. For example, in multi-photon microscopy, the resolution of the microscope depends on the spot size of the focus, and the two-photon excitation efficiency (and hence the microscope sensitivity) depends on the pulse duration. As a result, a transform-limited pulse and diffraction limited spot size are usually desired. Ultrafast micro-machining has similar requirements. When spatiotemporal distortions are present, such as those that can result from lens aberrations, it is difficult to compress the pulse, and a two-dimensional, or a spatiotemporal pulse compressor is needed.

Most pulse measurement techniques [11, 12], can only measure the pulse's temporal intensity and phase averaged over the focused spot size and therefore yield no information about the spatiotemporal couplings. Two-dimensional spectral interferometry (2DSI), and variations on holography can be used to measure the spatiotemporal field of an ultrashort pulse[13-15], but these measurements cannot be made directly at the focus. These techniques can be used to indirectly characterize focused pulses by measuring the spatiotemporal field of the recollimated beam and then numerically back propagating this field to the focus[14]. The disadvantage to this approach is that the recollimation must be perfect and the numerical method for back propagating has to be trusted.

The technique of Interferometric Photon Scanning Tunneling Microscopy can measure the spatiotemporal field of ultrashort pulses with high spatial resolution[16-19], although this technique has never been used to measure focusing pulses. Also, this technique is a time-domain linear-interferometric technique, so it has the disadvantage that scanning is required to obtain temporal information.

Recently we introduced a simple and convenient method for directly measuring the spatiotemporal field of focusing ultrashort pulses, which is a variation on a technique we developed, called SEA TADPOLE, or Spatially Encoded Arrangement for Temporal Analysis by Dispersing a Pair of Light E-fields[20-22]. SEA TADPOLE is an experimentally simplified *and* high-spectral-resolution version of spectral interferometry[23]. SEA TADPOLE is a linear optical techniques that involves temporally overlapping and crossing the unknown pulse with a reference pulse in order to measure $E(\omega)$ for pulses that are potentially complicated (in time or frequency), such as shaped pulses. Fiber optics are used to introduce the beams into the device, which makes it easy to align. Using crossed-beams allows $E(\omega)$ to be retrieved without losing spectral resolution[24-27], so that very complicated, long pulses can be measured. Using SEA TADPOLE, we have been able to measure pulses with time-bandwidth products of 400 [22].

Because the entrance to SEA TADPOLE is a single-mode optical fiber, it also has spatial resolution, which is limited only by the fiber mode diameter (in our initial work, we used a fiber with a 5.4-μm diameter). By scanning the fiber in space and making many measurements of $E(\omega)$ at different positions all along the focusing beam's cross section, we have used this device to measure the spatiotemporal electric field of pulses [21]. As long as the focus to be measured has a numerical aperture (NA) less than that of the fiber, SEA TADPOLE has sufficient spatial resolution and acceptance angle to measure the spatiotemporal electric field of a focusing pulse. This has allowed us to measure the spatiotemporal field of focused pulses with NA's of up the 0.12 or with focused spot sizes larger than 5.4μm.

Here we introduce a new version of SEA TADPOLE, which uses an NSOM (Near Field Scanning Optical Microscopy) fiber probe in place of the single mode optical fiber to extend our spatial resolution to be < 1 μm [28, 29]. NSOM has been used in the past to measure the spatial intensity distribution of tightly focused continuous-wave lasers[30]. Using an NSOM probe with an aperture diameter of 500 nm, we have measured $E(x,y,z,t)$ for focused pulses

with NAs as high as 0.44 and features in their intensity < 1 μm. Using this device we observe some of the severe focused-pulse distortions previously predicted, but never directly observed, such as radially varying group-delay dispersion, an "X-shaped pulse", and the "forerunner pulse."

2. Experimental setup

To measure $E(\lambda)$ at one position, a reference pulse is coupled into a single-mode optical fiber, and the focusing pulse is sampled with a nearly-identical fiber that has an NSOM probe at its sampling end. At their outputs, the two fibers are placed on top of one another, and the light diverging from the two fibers is collimated with a single lens. This not only collimates the beams, but also causes them to cross so that they interfere, and we place a camera at the crossing point to record their interference. In the other transverse dimension, a lens maps wavelength onto the horizontal position of a camera, so that he camera records a two-dimensional trace $I(x_c,\lambda)$, where x_c is the camera pixel along the vertical dimension. The electric field of the unknown pulse at that NSOM probe position is then reconstructed using Fourier filtering along the x_c axis, as described in references[20, 22, 27].

To measure the spatio-temporal electric field of a focusing ultrashort pulse we mount the NSOM probe end of the fiber to an x-y-z scanning stage as illustrated in Fig.1.
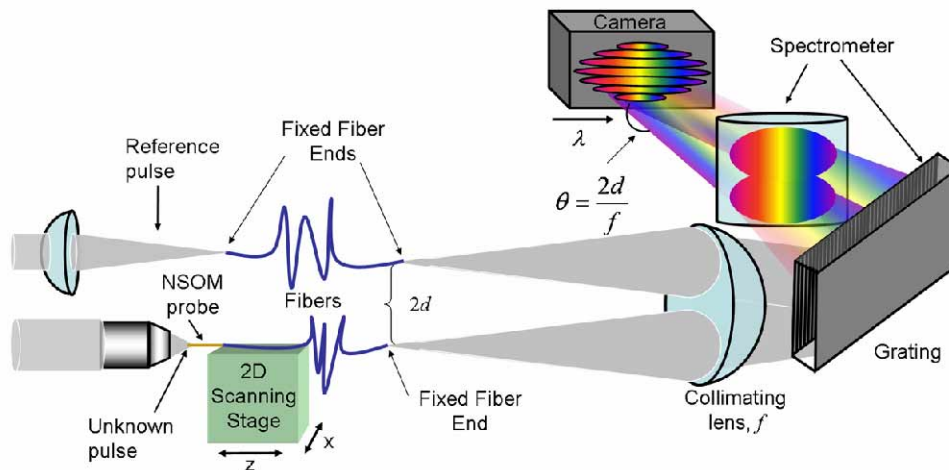

Fig. 1. NSOM-Scanning SEA TADPOLE experimental setup: An NSOM fiber samples the focusing pulse. The reference pulse is coupled into an identical fiber without an NSOM probe on its end. At the outputs of the fibers, the diverging beams are collimated using a spherical lens (f). After propagating a distance f, the collimated beams cross, and a camera records the resulting interference. In the other dimension, a grating and a lens map wavelength onto the camera's horizontal axis (x_c). The NSOM probe is scanned in x and z, so that $E(x,z,\lambda)$ is measured.

The NSOM probe must have an aperture diameter smaller than the focus so that it collects light from the focusing beam over a small area (given by the area of the aperture), or essentially at one point within the focus. This allows us to measure an interferogram at many positions of the focusing beam by scanning the NSOM tip longitudinally and transversely, so that we can measure an interferogram at many locations within the focus. From each interferogram we reconstruct $E(\lambda)$ for its corresponding location, which yields (after Fourier transforming to the time domain) $E(x,y,z,t)$ around the focus, just as we did with the single-mode fiber in our previous work[21].

The NSOM fiber probes that we use were purchased from Nanonics. These are made by tapering one end of a single mode fiber (the fiber is the same kind of fiber that we use in the reference arm). The end of the taper is coated using chromium and gold and a small aperture or hole is left uncoated. In our experiments so far, we have used probes with aperture diameters of 500 nm and 1 μm because these were sufficient to measure the pulses that we were interested in. Though in principle, even the smallest aperture NSOM probes could be used in SEA TADPOLE to achieve even higher spatial resolution.

SEA TADPOLE, like all linear interferometers, measures the spectral-phase difference between the two arms of the interferometer. The phase of the reference pulse can be removed from this difference to isolate the phase of the unknown pulse. Or if one is interested in the phase introduced by some element that is in the unknown arm of the interferometer, then the phase difference will provide this. In this work, we desire the spectral phase introduced by a lens (at every position within the focus), so, from each interferogram, we retrieve the spectral-phase difference between the two arms of the interferometer.

3. Characterizing the NSOM probes

As discussed previously[20, 21], when sampling a focusing beam, the aperture diameter must be smaller than the focused spot size. This simultaneously provides sufficient spatial resolution and acceptance angle. Thus, a small enough NSOM probe will accurately spatially resolve the focusing pulse and collect all of the k-vectors from the focus [20].

Because NSOM fiber probes are difficult to manufacture and easy to damage, it is important to characterize the probe (that is, measure its transfer function) before making any measurements to assure that the probe will not introduce artifacts in the measurement, and this characterization can be done is several different ways (for example see [29]).

Here we make the measurement by sending a collimated Gaussian beam into the small probe end and measuring the transmitted intensity as a function of the angle that the probe's axis makes with the beam's axis[31]. Because the Gaussian beam is 1000 times or more larger than the probe diameter, it is essentially a plane wave and, therefore, any change in intensity with angle, is due to the NSOM tip transfer function. We only measured the one-dimensional transfer function and so only rotated the probe in the plane of the table. This was sufficient for our measurements (see section 4) of focusing pulses due to the rotational symmetry present

Figure 2 shows the results of this measurement for two different NSOM fiber probes.
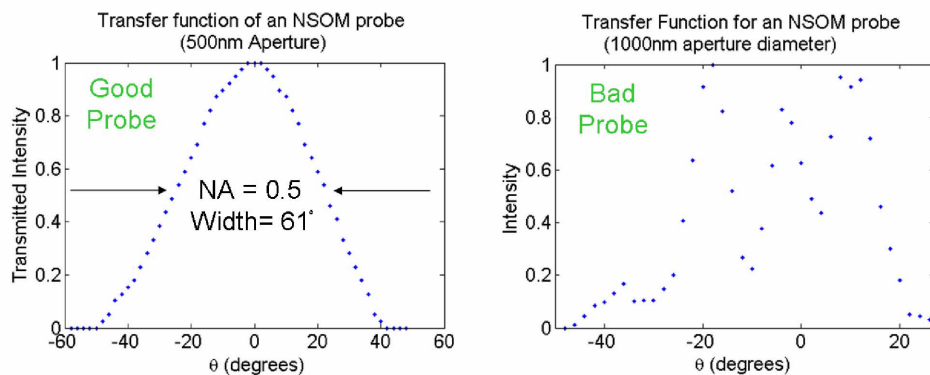

Fig. 2. Measured transfer function for two different NSOM fiber probes. Each measurement shows the power transmitted through the NSOM probe as a function of the incidence angle of the input beam. Left: An NSOM probe that is suitable for out measurements and has an NA of 0.5. Right: A damaged NSOM probe that would k-vector-filter the focusing pulse in a complicated and unacceptable way.

The image on the right shows the transfer function for a 1μm probe that has a very complicated transfer function. This probe would angularly filter the focusing pulse in a complicated way and is therefore not suitable for our measurements. This probe was likely bumped and damaged. The measurement on the left shows a much smoother and broader transfer function. As we have discussed earlier, provided that the NA of the focused beam is less than the NA of the sampling NSOM fiber probe (which we took to be the sine of the half width at $1/e^2$ of the maximum of the transfer function), the probe will collect essentially all of the k-vectors of the light at the given point in space and therefore will sample the beam reasonable well[21]. Therefore, using this probe we can measure foci with numerical apertures less than 0.5. The transfer function shown on the left was smoothed using a window size of 3 points to remove measurement noise.

Because this is an intensity measurement, it will not tell us if the transfer function is complex (has variations in its imaginary component), which would correspond to a variation in the phase of the light collected as a function of angle. A badly distorted probe (such as the one shown on the right of Fig, 2), which is not perfectly opaque outside of the aperture, could have a complex-valued transfer function. But as long as the NSOM probe really is an aperture, then its transfer function should be purely real. The measured transfer function for the 500-nm aperture indicates that this NSOM probe is not distorted, and therefore it is safe to assume that its transfer function is, not only smooth and broad, but also real. Our results corroborate this conclusion (see section 4).

Another potential source of error in our measurements is spectral filtering of the collected light by the NSOM probe (the probe could, in principle, collect some colors more efficiently than others), but we made spectral transmission measurements, as well, and confirmed that ours did not. Previous papers have also reported that NSOM probes do not change the spectrum as long as the power is low enough to avoid nonlinear effects, which it is here[32, 33].

4. Experimental results

Using the 500-nm-aperture diameter NSOM fiber probe that we characterized (shown on the left in Fig.2) above, we measured the spatiotemporal field of foci from several different lenses in order to test our method.

In all of these measurements, we used our KM Labs Ti:Sa oscillator, which had a bandwidth of 20 nm (FWHM) or 50 nm for the X-pulse measurement, and we never introduced more than 10 mW into the NSOM probe (as suggested by Nanonics) to avoid damaging it. As explained in section 2, because we measure the phase introduced by the lens, any spectral phase that the input pulse has, cancels in the measurement and the pulse that we measure is effectively transform limited before the lens (47fs, or 19fs). The temporal resolution in our measurement is given by the inverse of the spectral range of the spectrometer and this was 12fs, though we generally zero fill the spectral electric field before Fourier transforming to the time domain using around 1000 zeros to smooth out the measured temporal intensities. The beam and all of the lenses that we used had rotational symmetry, so measuring $E(x,z,t)$ was sufficient to test our method, and we only measured $E(x,z,t)$, although we can also easily scan in y in the future if necessary. To scan the NSOM probe, we used motorized actuators, which had a minimum step size of 200 nm or better. All other experimental details for SEA TADPOLE can be found in previous references[20-22].

4.1 Microscope objectives

As our first experimental test, we focused the beam using two different aberration corrected microscope objectives and measured $E(x,z,t)$ at and around the focus (or the point where the beam had its smallest spot size). Because the parameters for these objectives are proprietary,

we could not perform simulations to verify these results. But, even though these objectives are designed for the visible, they have significantly less aberrations than singlet lenses and instead have significant group delay dispersion (GDD) due to the large amount of glass in their multiple elements [8]. Therefore we made these measurements to verify that the focus from the microscope objectives that we measured showed a relatively smooth, small, and flat pulse front (as determined by previous simulation [8]), which would indicate that the NSOM probe was accurately sampling the focusing beam. The pulse fronts for this measurement (and for the 20x objective) are flat because the measurements were made so close to the focus.

The first objective that we used was a 10x (f = 16.5 mm, clear aperture diameter = 7.5 mm) microscope objective, and Fig. 3 shows the results of this measurement.
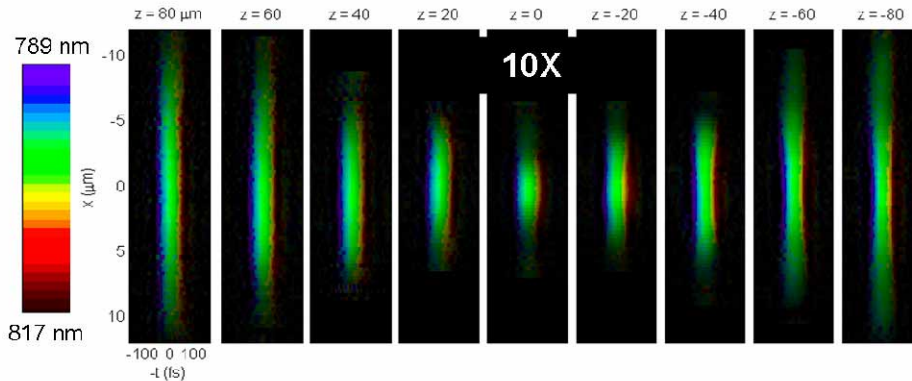

Fig. 3. Measured $E(x,z,t)$ for a pulse focused with a 10x microscope objective. Each box shows the $E(x,t)$ at a certain distance from the focus (z) which is written above the box. The (false) color in the plot is the instantaneous frequency of the pulse as indicated by the color bar.

Each box in Fig. 3 shows the pulse's amplitude as function of t and x (the transverse position) at a certain distance from the focus (or the point where then beams spot size was the smallest). The color in the plot shows the instantaneous frequency of the pulse as indicated by the color bar.

The main distortion seen in the focus is that the redder colors precede the bluer colors, or that the pulse is chirped, as expected from the GDD introduced by the multi-element, aberration-corrected refractive lens. Interestingly, the center part of the beam is more chirped than the sides—due to the radially varying GDD—which is also expected considering that the center of the objective contains more glass than the sides (especially apparent at $z = -40$ and -20). Other than these two distortions, the pulse front is fairly smooth, as expected. The spot size of the intensity averaged over time at the focus of this objective has a FWHM of 3μm.

We measured the focus of a similar, but higher NA, objective (20x, f = 9 mm, clear aperture diameter = 6 mm), and the results of this measurements are shown in Fig. 4.
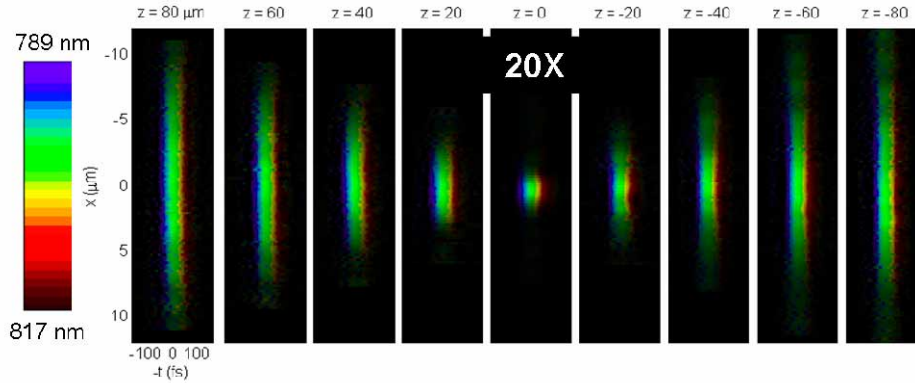
Fig. 4. Measured $E(x,z,t)$ for a pulse focused with a 20x microscope objective. Each box shows the $E(x,t)$ at a certain distance from the focus (z) which is written above the box. The color in the plot is the color of the pulse as indicated by the color bar.

As with the 10x objective, the main distortion seen in the focused pulse is chirp. The pulse from this objective looks more chirped than that from the 10x objective which is expected considering that a higher NA objective probably contains more glass. Also, the focused spot of the intensity averaged over t had a FWHM of 1.8μm.

In both of the above measurements, we focused the ~1mm beam directly out of the oscillator, which we routinely monitor using a Swamp Optics GRENOUILLE, which shows it to be free of pulse-front tilt and spatial chirp. As in previous work, our measurements confirm that this beam was also free of other spatiotemporal distortions [20, 21, 34]. Were this not the case, then our SEA TADPOLE measurements would show these distortions as well as those introduced by the lens.

Finally, because the beam was much smaller than the clear aperture of the objectives, no edge diffraction effects are seen in these measurements.

4.1 Singlet lenses

For the next two measurements, we used a telescope to increase the beam's spot size by a factor of four, yielding a FWHM of 4 mm at the focusing lens. To ensure that minimal aberrations were introduced by the telescope we put a 25-μm pinhole at the focus of the telescope to spatially filter the beam. This filter also removed any spatiotemporal distortions that may have been present before the telescope. The telescope consisted of two plano-convex lenses with focal lengths of 100 mm (25-mm diameter) and 400-mm (50-mm diameter). The spatial filter did not remove any aberrations introduced by the second lens (the 400mm focal length lens), but because this lens has such a low NA, its aberrations are negligible.

To test our measurements, we also numerically propagated the fields through these lenses using all of the experimental parameters. We performed the simulations using the method described in this reference[8], which does not use the paraxial approximation and is therefore valid as long as the scalar approximation is valid or for NAs up to 0.7. We assumed that the field was Gaussian in time and space, so minor discrepancies between the simulations and the measurements could have been due to this assumption.

We measured $E(x,z,t)$ for a pulse focused using an SF11 plano-convex lens, with a diameter of 12 mm and a focal length of 12 mm. The NA of this focus was 0.28 (using the standard definition for Gaussian beams, which is the radius of beam at $1/e^2$ of its peak

intensity, divided by the focal length). Figure 5 shows the results of this measurement at the top, and the results of the simulations are shown at the bottom.
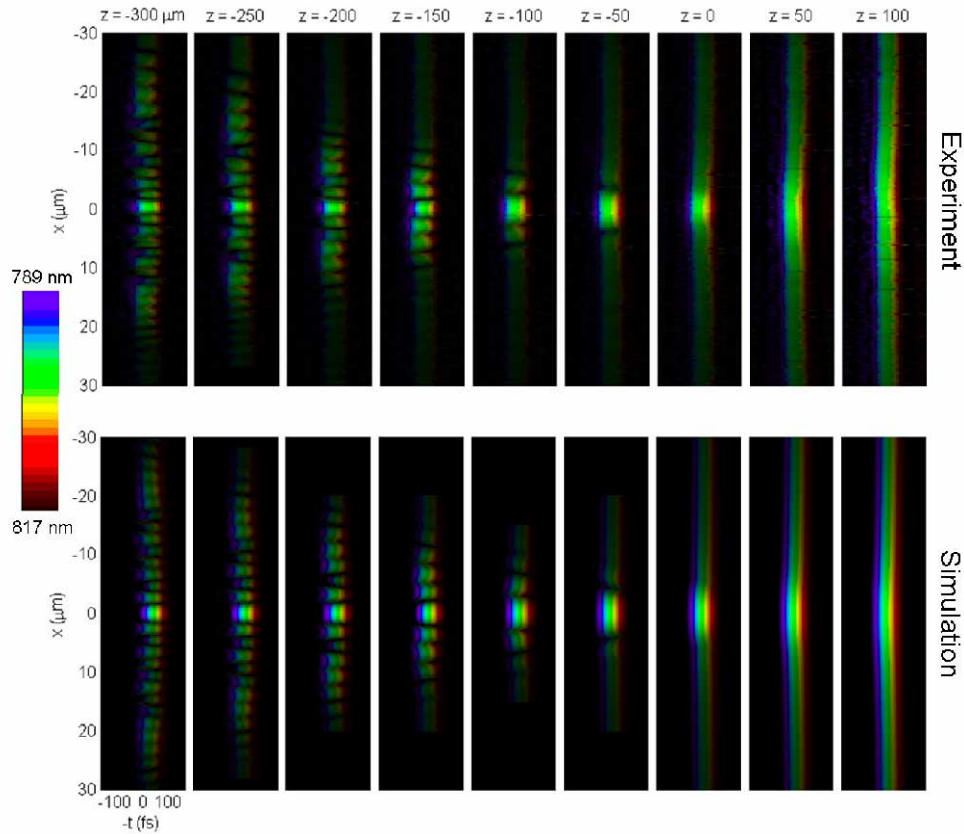

Fig. 5. Measured $E(x,z,t)$ for a pulse focused with a 0.28 NA SFll plano-convex lens. Each box shows the $E(x,t)$ at a certain distance from the focus (z), written above the box. Redder colors precede bluer ones in time due to the material dispersion introduced by the lens. The ripples that appear before the focus are due to spherical aberrations. The smallest features in the data have a width of 1 μm, which illustrates our spatial resolution.

The results shown in Fig. 5 show good agreement between the simulation and the experiment. In these plots, z = 0 is defined as the geometric focus, which we find using the simulations. Because of the material dispersion introduced by the lens, the redder colors precede bluer colors. The ripples that are seen before the focus are due to the large spherical aberrations. The smallest of these ripples has a width of 1 μm (looking at the FWHM of a ripple in the intensity versus *x* at one *t*), which illustrates our high spatial resolution.

We also measured a pulse focused with a similar plano-convex lens made of BK7 with a focal length of 15 mm and a diameter of 12 mm. The purpose of this measurement was to observe the Bessel-like X-shaped pulse that occurs before the geometric focus due to spherical aberrations[5]. The BK7 lens has about the same amount of spherical aberration as the SF11 lens, but much less GDD (by a factor of ~ 3), which makes it easier to observe this distortion. We also increased the bandwidth of our laser to 50 nm (FWHM) when making this measurement.

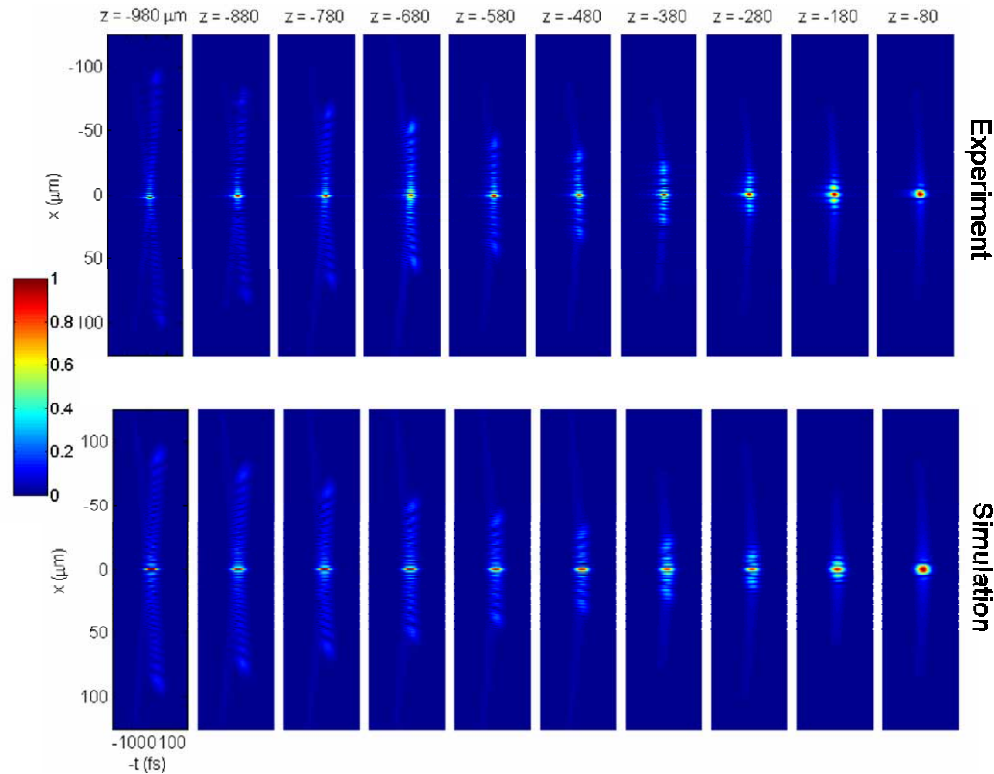Figure 6 shows the results of the simulation and the measurement for this focus.

Fig. 6. Measured $|E(x,z,t)|$ for a pulse focused with a 0.28 NA SFll plano-convex lens. Here the results are plotted using color to represent the intensity as indicated by the color bar and the phase information of this pulse is not shown here.

For this measurement we plotted $|E(x,z,t)|$ (the amplitude as opposed to the intensity) of the focusing pulse and not the phase so that the shape of the pulse could be more easily seen. The color in these plots represents the normalized intensity as indicated by the color bar. The phase of this pulse simply showed that there was positive GDD and we found good agreement between the simulations and the measurements for this.

The measurements and the simulations shown in Fig. 6 for the intensity are in good agreement; both show the presence of a Bessel-like pulse between 0.9 and 0.5 mm before the geometric focus. As reported in a previous theoretical paper, extreme spherical aberrations result in a Bessel-like pulse (characterized by the "X-shape") between the marginal (z=-3mm) and the paraxial focus (z = 0)[5, 8]. As far as 0.9mm away (and all the way to the marginal focus) from the geometric focus, most of the pulse's energy is confined within a 1-µm spot size. It is also interesting to note that the "X-shaped" part of the pulse travels faster than the main pulse front and therefore faster than the speed of light. This is allowed because the "X-shaped" intensity pattern is due to interference, so it does not carry any energy[8]. This pulse is different from a real Bessel pulse because its spatiotemporal shape and speed of propagation change a little as it propagates, and the Bessel-like pulse only exists between the paraxial and the marginal foci[8].

The next measurement that we made was of the focus produced by a New Focus aspheric lens made of CO550 glass with a focal length of 8 mm, an aperture diameter of 8 mm; the focus had an NA of 0.44. To determine the aberrations in this lens for the simulations, we performed ray tracing using OSLO[35] and used the lens parameters provided by New Focus. Because this lens is designed to be used with a glass cover slip, which we did not use in our

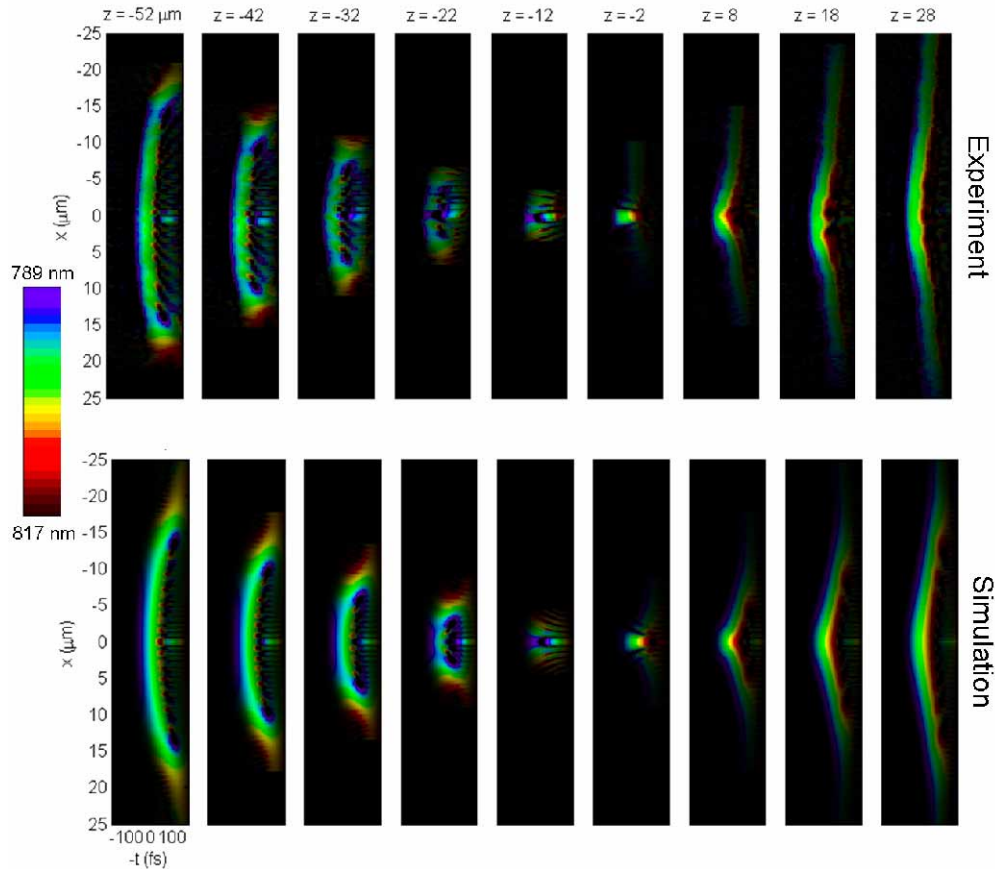experiment, some spherical aberrations are present. Figure 7 shows the results of the measurement.

Fig. 7. Measured $E(x,z,t)$ for a pulse focused with a 0.44 NA aspheric lens. Each box shows $E(x,t)$ a certain distance from the focus (z) written above the box. In addition to the distortions seen in our previous measurements, here the color also varies along the x direction due to the severe chromatic aberrations that are present. The combination of overfilling the lens and chromatic aberrations result in the additional "fore-runner" pulse ahead of the main pulse before the focus.

Again, the results of the simulation and the experiment are in good agreement. The color varies with time due to GDD and also with the transverse position x due to chromatic aberrations. Also the redder colors focus later than the bluer colors, so before the focus the blue is at the center and the red is on the edges of the pulse.

The most striking feature in this data is the presence of the additional pulse, the so called "fore-runner pulse" than can be seen before the focus. This additional pulse results from the combination of diffraction at the edge of the lens and chromatic aberration[3, 8]. The "fore-runner pulse", like the "x-shaped" pulse, travels faster than the main pulse front meaning that it is traveling faster than the speed of light. Again, because this additional pulse is the result of interference, it does not carry any energy, so this does not violate the theory of relativity[8]. The FWHM of the intensity of the additional pulse is less than 1μm. The small amount of spherical aberration present in this focus increases the intensity of the additional pulse.

Due to chromatic aberration, the color of the pulse also changes as it propagates. To better visualize this, we made a movie of this pulse focusing by streaming together 21 measurements and using interpolation to generate 150 frames. The movie is shown in Fig. 8.
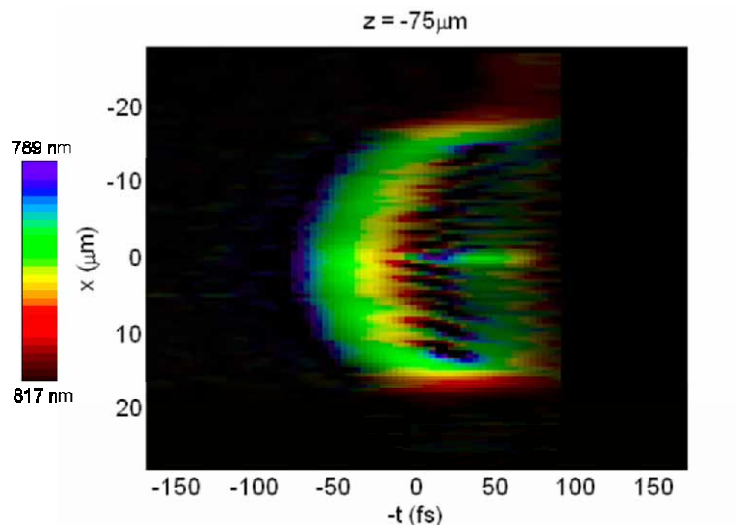

Fig. 8. (Media 1) Movie of a focusing pulse from the 0.4 NA aspheric lens: Due to the severe chromatic aberrations, the pulses' color varies in *x*, *t*, and *z*.

The movie is shown from the prospective of someone moving along beside the pulse as it focuses. Note that the center of the pulse color at its center changes from blue to green and then red as it propagates, because different colors are focusing at different values of z.

6. Other issues and comments

Each time that we moved the NSOM probe to a different z, we also adjusted the path length of the reference pulse so that there would always be zero delay between the two pulses. But in our measurements (which are automated), the adjustment did not always work perfectly, and the delay between the focusing pulse and the reference pulse was not zero for every value of *z*. At most it was off by ~100 fs. Because of the agreement between the simulations and the measurements, we believe that the location of the NSOM probe with respect to the focus (or the *z* value) is still correct (or very close), and that the varying delay was due to a drift in the reference arm of the interferometer or the inaccuracy of the stage that moves the reference pulse. Using the simulation as a reference, we recentered each *E*(*x*,*t*) on the time axis to the appropriate place. In the future, using better translation stages or adjusting the delay to be zero within our program, we should be able to fix this problem. We only had to make this adjustment for the aspheric lens data where we used a smaller step size in *z* than in any of the other measurements.

In all of our measurements, measuring *E*(*x*,*t*) at one *z* typically took about 1 min, so the measurements in Figs. 3-6 each required ~ 9 minutes, and the data for the movie required ~ 20 minutes to collect. Measuring the X-pulse required taking ~ 10 times as many points due to the small features present in the pulse's large wings, so the data shown in Fig. 6 required ~ 2 hours.

As we explained in our previous papers[20, 21], because we have not perfectly stabilized our interferometer, it experiences a slow phase drift that only affects the absolute spectral phase. This means that we cannot measure the spatial phase of the focusing pulse, but so far we have not been interested in the quantity, which is more relevant for monochromatic light than for pulses. But, we were able to match the measurements with simulations, and we know

the spatial phase from the simulations. On the other hand, SEA TADPOLE does measure the variation of *all* the higher-order spectral phase terms with *x* and *t*, such as the radially varying group delay (or the pulse front), the radially varying GDD, and the spectrum as a function of *x*, *y*, and *z*. If we ever need to know the spatial phase, we should be able stabilize the interferometer by building a box around it to isolate it from environmental factors that cause this drift [17], or it may be possible to extract the spatial phase from our data considering that we measure $E(x,t)$ at different *z*'s.

7. Conclusions

We introduced a method for measuring the spatiotemporal electric field of focusing ultrashort pulses with sub-micron spatial resolution, femtosecond time resolution, and high spectral resolution. We made these measurements using SEA TADPOLE with an NSOM fiber probe to spatially resolve the focusing pulse. We make multiple measurements of $E(x,t)$ at many positions throughout the focus by scanning the NSOM probe longitudinally and transversely in order to measure $E(x,z,t)$.

Before making any measurements, we measured the transfer function of several NSOM probes in order to find one that had a high enough numerical aperture and a smooth transfer function so that it would accurately indicate the focusing pulse at the point of interest. Then using this NSOM probe (the 500-nm diameter one shown in Fig. 2), we tested our technique by measuring the foci produced by two different microscope objectives. The primary distortion we saw in these foci was chirp as expected and we observed some radially varying GDD in these measurements.

We also measured $E(x,t)$ at and near the foci produced by two different plano-convex lenses (NA = 0.28, and 0.23) and an aspheric lens (NA = 0.44). To verify these measurements, we simulated these foci and found good agreement between the simulations and measurements. With the NA = 0.23 plano-convex lens, we observed the X-shaped Bessel-like pulse due to its spherical aberrations. From the measurement of the focus of the aspheric lens, we made a movie of the pulse focusing. In these measurements, we were able to spatially resolve features in the intensity smaller than 1 μm, and we observed the "fore-runner pulse"—the additional pulse that appears ahead of the main pulse before the focus, due to chromatic aberrations and overfilling the lens. To our knowledge, these are the first measurements of the spatiotemporal field of the Bessel-like due to spherical aberrations and the "fore-runner pulse."

The agreement between our measurements and simulations also verifies the validity of the non-paraxial simulations that we use for calculating the spatiotemporal field of focused ultrashort pulses which can be a very useful tool.

In the future using NSOM probes with even smaller apertures, we hope to measure even more tightly focused pulses such as those from the high NA objectives that are routinely used in microscopy.